Prediction of Micromixing Effects in Precipitation: Case of Double-Jet Precipitators

René David
Laboratoire des Sciences du Génie Chimique, CNRS-ENSIC-INPL, 54001 Nancy Cedex, France

Bruno Marcant
Rhône-Poulenc Recherches, 52, rue de la Haie-Coq, 93308 Aubervilliers Cedex, France

Mixing effects are evaluated for double jet semibatch and continuous stirred precipitators by a model which gives the variation of the primary nucleation flux from the mixing conditions. The predicted trends are compared with results of various authors, including those from a new study of calcium oxalate semibatch double-jet precipitation. Satisfactory qualitative agreement is found for the different chemical systems as a function of feed rate, stirring speed and feed locations for calcium oxalate precipitation. Two types of precipitation systems are demonstrated, depending on the ratio added/tank volume, the initial supersaturations and the intrinsic stiffness factor of a given precipitation. The difference between the two types depends on the increase or reduction of the primary nucleation flux by imperfect mixing with respect to the reference primary nucleation flux obtained with perfect mixing.

Introduction

In a recent article, Marcant and David (1991) presented a qualitative prediction for micromixing effects on precipitations in single-jet batch and semibatch precipitators. Their model suggested some general rules for the effects of mixing in the case of single-jet precipitators on calcium oxalate monohydrate:

- Micromixing effects are best avoided in contacting rapidly two equal volumes of reactants provided that the number of mols of reactants is kept constant.
- On the other hand, for a given stoichiometry, any increase of the initial volume ratio accentuates mixing effects.
- Having only a small volume available for micromixing counterbalances the high nucleation rates resulting from high intermediate local supersaturations. Consequently, uncomplete micromixing generally results in a smaller number of final crystals which accordingly have larger average sizes.
- Changes in the feed point location in stirred tanks have a more drastic effect on crystal number and sizes than modifications of the stirring speed.

This article is concerned with double-jet precipitators. Our objective is to study the combined influence of mixing parameters and primary nucleation on final crystal size and to examine if variations of the average crystal size may be predicted from a simple description of mixing. Few experimental results exist for double jets, and their interpretation is much more difficult because of the greater number of parameters involved.

Literature Survey

Some experimental results on double-jet precipitation in continuous or semibatch stirred tanks are reported in the literature (Kuboi et al., 1986; Tosun, 1988; Pohorecki and Baldyga, 1988; Fitchett and Tarbell, 1990). Mydlarz et al. (1991) have precipitated zinc oxalate in a mixed-suspension, mixed-product-removal (MSMPR) with premixing in a prenucleator. All these studies are listed in Table 1. In a detailed study by Tosun (1988), very pronounced mixing effects in barium sulphate precipitation were observed. Four different couples of symmetrical feed points were examined: in the setup called BB, the feed streams were symmetrically injected far from the Rushton turbine and far from one another. In setup AA, the feed streams were also symmetrically separated one from the other, but located both in the discharge stream of the turbine which is highly turbulent. In the third setup CC, both feed

Correspondence concerning this article should be addressed to R. David.

Table 1. Experimental Results for Double Jet Stirred Tanks vs. Model Predictions: I. Unchanged; II. Moderately Increased; III. Decreased; IV. Strongly Decreased; V. Intermediate Minimum

Authors	Mode	Tank Vol. (dm^3)	Var. of	Double-Feed Position	Exp. Parameters α (20–22)	Exp. Parameters B	Exp. Parameters σ^f	Exp. Effect on Avg. Particle Size	Model Pred. For ϕ
Kuboi et al. (1986) Barium Sulfate	Semibatch	6.2	Feed Loc.	Symmetrical Separated in Low Turbulence Region	400	220	1.7×10^8 to 7×10^8	III If Feed Tubes Were Brought Together	Zone *a* β I, γ II η II, ϕ II
Pohorecki and Baldyga (1988) Barium Sulfate	Cont. without Premixing	0.7	Stirring Speed	Symmetrical Separated in Low Turbulence Region	150	220	2.5×10^5 to 2.5×10^6	II With Increasing N	Zone *a* ?
			Space Time	Symmetrical Separated in Low Turbulence Region	50–250	220	2.5×10^5 to 2.5×10^6	III With Increasing τ	Zone *a* ?
Fitchett and Tarbell (1990) Barium Sulfate	Cont. without Premixing	1.8	Stirring Speed	Symmetrical Separated in Low Turbulence Region	10–80	220	4×10^6 to 10^9	I (Except $N=0$)	Zone *a* ?
Tosun (1988) Barium Sulfate	Semibatch	6	Feed Loc.	AA: Symmetrical Separated in High Turbulence Region	2,850 -28,500	220	10^{10}	II	Zone *b* at High N β II, γ I η II, ϕ II
				BB: Symmetrical Separated in Low Turbulence Region				Base Case	Zone *b* at High N Base Case
				DD or CC: Symmetrical in High Turbulence Region				IV	Zone *b* at High N β II, γ II η II, ϕ II
			Stirring Speed	AA-DD				V With Increasing N	Zone *b* at High N β II, γ I, α II η II, ϕ II
Mydlarz et al. (1991) Zinc Oxalate	Cont. With Premixing	0.5	Stirring Speed Space Time	Premixing	500 -6,000	?	15 to 35	III With Increasing N	Zone *b* β II, $\gamma=1$, α II η II, ϕ II
								V With Increasing τ	Zone *b* α II, η II, ϕ II

streams were side by side and located just below the turbine. In the fourth location DD, both feed tubes were above the turbine, but with a relative distance of D/2. For setup CC, the average crystal size was strongly reduced, whereas with setups AA and BB at stirring speeds ranging from 100 to 300 min^{-1}, approximately similar crystal-size distribution were obtained, with a slightly lower average size in the case BB. At higher stirring speeds, the average size was significantly lower in location BB. Surprisingly, setup DD always yielded much larger average sizes than setup CC at any stirring speed. When changing the stirring speed N, the crystal size passed through a minimum value at an intermediate value of N for all sets of feed points.

Evaluation of Possible Mixing Effects

As in the first article, let us consider a precipitation consecutive to a chemical reaction between two reactants A and B with respective feed concentrations C_A^f and C_B^f. For the sake of simplicity, we consider a stoichiometric 1-1 precipitation though the calculations can be easily derived for other stoichiometries:

$$A + B \rightarrow S_{solid}$$

Both feed streams are discretized over the feed time interval t^f in m fractions of respective volumes V_B^0 and $V_A^0 = \delta V_B^0$. These fractions are fed in the tank that already contains a volume αV_B^0 where the concentrations of species A and B are C_A^b and C_B^b (Figure 1) respectively. In the absence of reactive conversion, complete and perfect mixing of these fractions with the bulk would give the concentrations C_A° and C_B°:

$$C_A^\circ = \frac{\delta C_A^f + \alpha C_A^b}{1+\alpha+\delta} \quad \text{and} \quad C_B^\circ = \frac{C_B^f + \alpha C_B^b}{1+\alpha+\delta} \tag{1}$$

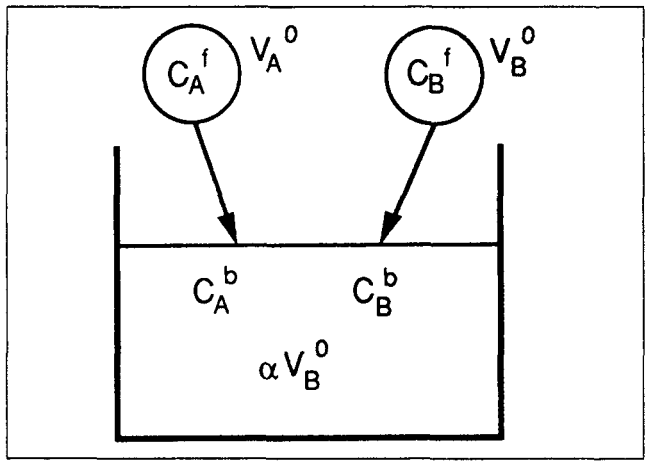

Figure 1. Mixing experiment.

and the corresponding supersaturation ratio:

$$\sigma^\circ = \frac{\sigma^b\left(\alpha + \frac{C_B^f}{C_B^b}\right)\left(\alpha + \frac{\delta C_A^f}{C_A^b}\right)}{(1+\alpha+\delta)^2} \tag{2}$$

with $$\sigma^b = \frac{C_A^b C_B^b}{P_S}$$

We envision the mixing process, as indicated in Figure 2, and assume that the important competing step in the mixing process is the primary nucleation consecutive to molecular contacting between reactive species. Due to the small size of nuclei, primary nucleation induces no significant consumption of reactants. It is also assumed that no significant consumption of fresh reactants occurs during the short mixing phase due to other processes such as growth, agglomeration, breakage or secondary nucleation. Growth, agglomeration, breakage and secondary nucleation are supposed to be slow with respect to primary nucleation. Of course, the final crystal-size distribution at the end of the whole precipitation is determined by all these processes.

Most of the A and B molecules reach the state of molecular contacting between reactive species before complete spatial distribution, that is, macromixing of the two fresh feed streams into the bulk. Molecular contact occurs on the one hand between one fraction of each fresh fluid stream and the bulk, and on the other hand between the rests of the fresh fluid streams together (Figure 2). Therefore, accounting for direct contacting between feed streams, we assume that a fraction γ_B of V_B^0, instead of being entirely mixed with the bulk of the tank, is mixed down to molecular level with the other fresh reactant A and a volume $\beta_I(\gamma_B+\gamma_A\delta)V_B^0$ of the bulk. The remaining fraction $1-\gamma_B$ is mixed with a volume $(1-\gamma_B)\beta_{III}V_B^0$ from the bulk alone (Figure 2). V_A^0 is also divided into two fractions, one of volume $\gamma_A V_A^0$ being mixed with fresh B and the bulk as indicated above, the other $(1-\gamma_A)V_A^0$ being mixed with $(1-\gamma_A)\beta_{II}V_A^0$ of the bulk. These three mixing subregions are numbered I, II, III respectively, as indicated in Figure 2.

Moreover, it is obvious that:

$$\beta_I(\gamma_B+\gamma_A\delta)+\beta_{III}(1-\gamma_B)+\delta\beta_{II}(1-\gamma_A)\le\alpha \tag{3}$$

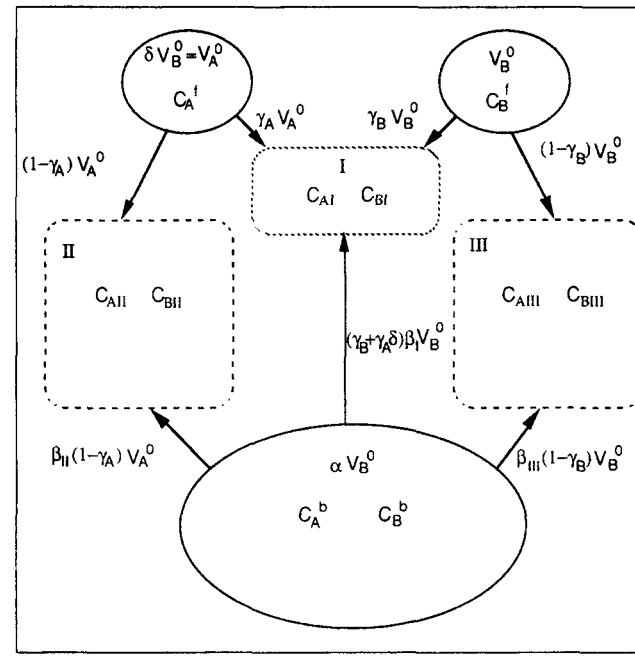

Figure 2. Mixing model.

The mixing concentrations in subregions I, II and III are the following:

$$C_{AI} = \frac{\beta_I(\gamma_B+\gamma_A\delta)C_A^b + \gamma_A\delta C_A^f}{(\gamma_B+\gamma_A\delta)(1+\beta_I)}$$

and

$$C_{BI} = \frac{\beta_I(\gamma_B+\gamma_A\delta)C_B^b + \gamma_B C_B^f}{(\gamma_B+\gamma_A\delta)(1+\beta_I)} \tag{4}$$

$$C_{AII} = \frac{\beta_{II}C_A^b + C_A^f}{1+\beta_{II}} \text{ and } C_{BII} = \frac{\beta_{II}C_B^b}{1+\beta_{II}} \tag{5}$$

$$C_{AIII} = \frac{\beta_{III}C_A^b}{1+\beta_{III}} \text{ and } C_{BIII} = \frac{\beta_{III}C_B^b + C_B^f}{1+\beta_{III}} \tag{6}$$

and thus the corresponding supersaturation ratios can be written as follows:

$$\sigma_I = \frac{\sigma^b\left[\beta_I(\gamma_B+\gamma_A\delta)+\gamma_A\frac{\delta C_A^f}{C_A^b}\right]\left[\beta_I(\gamma_B+\gamma_A\delta)+\gamma_B\frac{C_B^f}{C_B^b}\right]}{(\gamma_B+\gamma_A\delta)^2(1+\beta_I)^2} \tag{7}$$

$$\sigma_{II} = \frac{\sigma^b\beta_{II}\left(\beta_{II}+\frac{C_A^f}{C_A^b}\right)}{(1+\beta_{II})^2} \tag{8}$$

$$\sigma_{III} = \frac{\sigma^b\beta_{III}\left(\beta_{III}+\frac{C_B^f}{C_B^b}\right)}{(1+\beta_{III})^2} \tag{9}$$

We assume that the primary nucleation rate in any subregion

where the supersaturation σ is given by Volmer and Weber's (1926) relationship:

$$r_N = A_N \exp\left(-\frac{B_N}{\log_e^2 \sigma}\right) \tag{10}$$

Values of B_N of the order of 1 indicate heterogeneous primary nucleation, whereas values about 100 to 1,000 are characteristic of homogeneous primary nucleation (Dirksen and Ring, 1991).

The complete fluid volume is $(1+\alpha+\delta)V_B^0$; thus, we can evaluate the nucleation flux in the entire mixer for perfect instantaneous mixing as:

$$\phi^\circ = (1+\alpha+\delta)V_B^0 r_N^\circ \tag{11}$$

The corresponding flux for the case of nonperfect mixing is:

$$\phi = V_B^0\{\alpha - \beta_{III}(1-\gamma_B) - \delta\beta_{II}(1-\gamma_A) - (\gamma_A\delta+\gamma_B)\beta_I\} r_N^b + (\gamma_A\delta+\gamma_B)(1+\beta_I)r_{NI} + \delta(1+\beta_{II})(1-\gamma_A)r_{NII} + (1+\beta_{III})(1-\gamma_B)r_{NIII}) \tag{12}$$

We now define a criterion to account for the difference between the nucleation fluxes for real and perfect mixing relative to the same injected volume V_B^0:

$$\eta = \frac{\phi - \phi^\circ}{A_N V_B^0} \tag{13}$$

This criterion is preferred to the ratio $\xi = \phi/\phi^\circ$ (Marcant and David, 1991), because for some sets of parameters, the values of ϕ and ϕ° differ from more than ten or twenty orders of magnitude, ϕ or ϕ° being so low that the corresponding nucleation rate becomes meaningless. A positive value of η means that primary nucleation is enhanced with respect to the perfect mixing case. Conversely, a negative value of η means that primary nucleation is decreased with respect to the perfect mixing case. Note that ϕ° does not depend on β_I, β_{II}, β_{III}, γ_A and γ_B.

In order to reduce the large number 11 of parameters B_N, σ^b, α, δ, β_I, β_{II}, β_{III}, γ_A, γ_B, C_A^f/C_A^b, C_B^f/C_B^b of the general model we may assume that:

(1) The concentrations in the bulk are at equilibrium, that is:

$$C_A^b = C_B^b = P_S^{1/2} \text{ or } \sigma^b = 1 \tag{14}$$

As a consequence r_N^b is zero.

(2) The feed is stoichiometric:

$$C_B^f = \delta C_A^f \tag{15}$$

(3) The feed is symmetrical:

$$\gamma_A = \gamma_B = \gamma \text{ and } \beta_{II} = \beta_{III} = \beta \tag{16}$$

(4) When final molecular mixing with the bulk occurs, the previously premixed portions of feed fluid receive the same proportion of bulk fluid of the unmixed portions. This may be understood in the following way: If neighboring feed streams premix, they build a transient "emulsion-like" fluid phase which is finally mixed up to molecular level with the bulk in the same way as would separate feed streams.

$$\beta_I = \beta_{II} = \beta_{III} = \beta \tag{17}$$

Introducing:

$$\sigma^f = \frac{C_A^f C_B^f}{P_S}, \tag{18}$$

then reduces the problem to the six parameters B_N, σ^f, α, δ, β, γ if we consider that:

$$\frac{C_A^f}{C_A^b} = \left(\frac{\sigma^f}{\delta}\right)^{1/2} \text{ and } \frac{C_B^f}{C_B^b} = (\sigma^f\delta) \tag{19}$$

Results from the Model

The first result of the calculations is that the sign of η is found to be roughly independent of the β and γ values. Consequently, this sign depends mainly on σ^f, α, δ and B_N. A schematic representation of the behavior of double-jet precipitation is given in Figure 3 for $\delta = 1$. The (σ^f, α, B_N) plane is divided into two zones by the surface Σ, where Σ is the locus of the points where $\eta = 0$. Iso-B_N and iso-σ^f curves, as well as the intersection with the $\alpha = 1$ plane, are drawn in solid or dotted lines. The concavity of Σ covers the zone where the nucleation flux is decreased by nonperfect mixing (zone *a*; $\eta < 0$); on the other hand, deviations to perfect mixing enhance the nucleation flux outside of Σ (zone *b*; $\eta > 0$). Note that the existence of Σ also means that there are model conditions with partial mixing (β and $\gamma > 0$) where the nucleation flux is the same as the flux for perfect micromixing.

The influence of the two last parameters β and γ is shown in the two examples given in Figures 4-7 corresponding to zones *a* (Figures 4-5) and *b* (Figures 6-7), respectively. In zone *a*, the most sensitive parameter is β (except for $\gamma > 0.1$). An

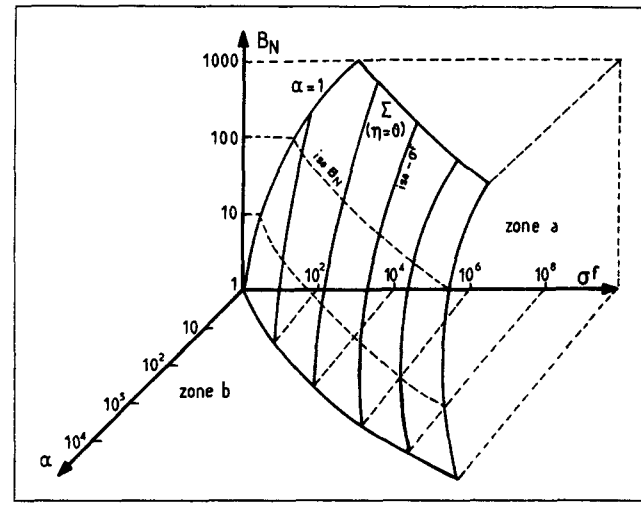

Figure 3. Influence of parameters α, σ^f and B_N on primary nucleation efficiency η.

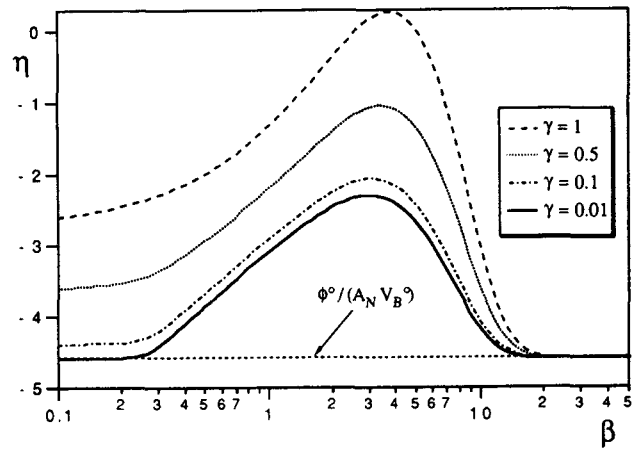

Figure 4. Influence of parameter β on the nucleation efficiency η; zone *a* conditions.

$\phi^\circ/A_N V_B^0 = 4.6$, $\alpha = 10$, $B_N = 1$, $\sigma' = 10^2$; $\beta = 5$ corresponds to the interaction of $V_A^0 + V_B^0$ with the entire tank.

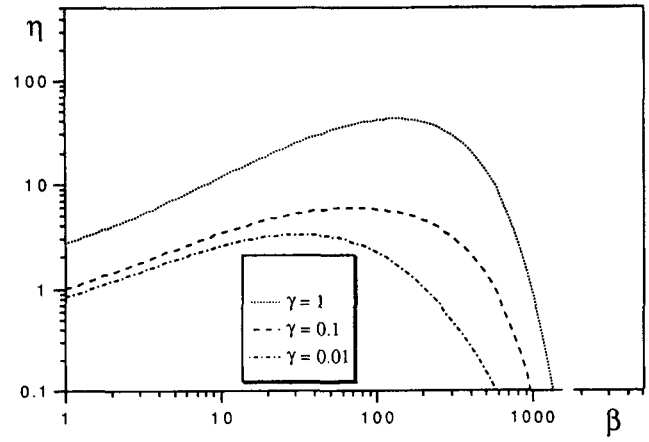

Figure 6. Influence of parameter β on the nucleation efficiency η; zone *b* conditions.

$\phi^\circ/A_N V_B^0 = 2.45 \times 10^{-19}$, $\alpha = 10^4$, $B_N = 100$, $\sigma' = 10^8$; $\beta = 5{,}000$ corresponds to the interaction of $V_A^0 + V_B^0$ with the entire tank.

increase of β results in a reduction of the absolute value of the negative nucleation criterion η. β is also the main parameter in zone *b* as the effect of increasing γ on η is only sensitive when $\gamma > 0.01$. An increase of γ always leads to a higher nucleation efficiency, whereas a β increase at constant γ induces an intermediate maximum for η. This maximum behavior results from two opposite effects when β increases: on one hand, the high supersaturation in subregion I is lowered; and, on the other hand, subregion I is expanding.

What does this mean in practice? Making γ higher means closer contact and deeper interaction between both jets, whereas increasing β means a better mixing of each jet separately with the bulk. $\beta = \alpha/(1+\delta)$ signifies that the complete volume αV_B^0 initially present in the tank participates to one of the three mixing subregions. Perfect mixing corresponds to a situation with $\beta = \alpha/(1+\delta)$ and $\gamma = 1$ (only subregion I).

In displacing both feed streams towards the stirrer, both β (higher local turbulence level) and γ (higher interaction between jets) may increase. But, when keeping them separated (γ low and constant), it should be possible to examine the effect of β alone. Under conditions of zone *a*, the nucleation flux will rise toward the perfect mixing limit. Under conditions of zone *b* this flux will first slightly increase and then decrease.

When the feed streams are put together (γ higher) but remain in the vicinity of the stirrer (β constant), the nucleation should be enhanced in any case and a larger number of crystals should be generated. These will attain a smaller final average size with the total mass crystallized being constant.

Ability of the model to represent double jet precipitation

The first point to be discussed concerning the question of whether this model is representative of the actual mixing and nucleation process is the reality of the interaction of mixing with primary nucleation. If we suppose that almost no consumption of the reactants takes place during the first seconds of the mixing process with the nuclei being too small, then the mixing is restricted to a linear mass exchange process from which local concentrations and supersaturations are given by the relationships 1-9. The nonlinearity is introduced by the

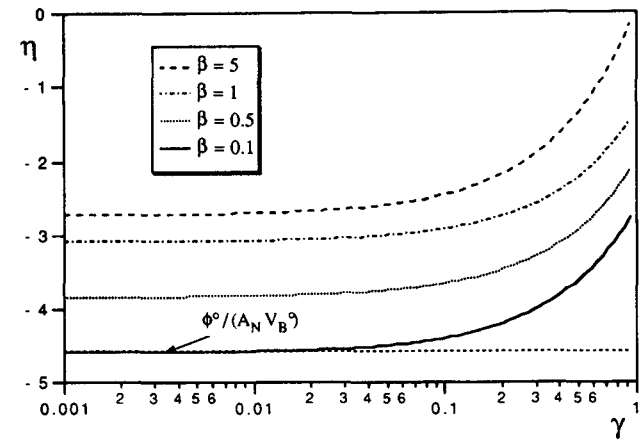

Figure 5. Influence of parameter γ on the nucleation efficiency η; zone *a* conditions.

$\phi^\circ/A_N V_B^0 = 4.6$, $\alpha = 10$, $B_N = 1$, $\sigma' = 10^2$; $\beta = 5$ corresponds to the interaction of $V_A^0 + V_B^0$ with the entire tank.

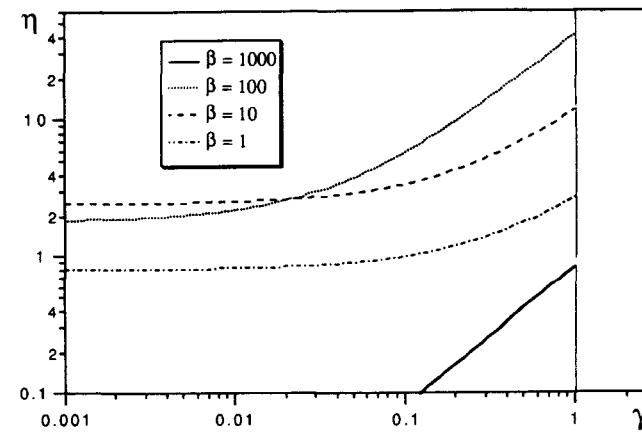

Figure 7. Influence of parameter γ on the nucleation efficiency η; zone *b* conditions.

$\phi^\circ/A_N V_B^0 = 2.45 \times 10^{-19}$, $\alpha = 10^4$, $B_N = 100$, $\sigma' = 10^8$; $\beta = 5{,}000$ corresponds to the interaction of $V_A^0 + V_B^0$ with the entire tank.

Volmer law (Eq. 10) which is monotonic. It is thus likely that the true overall nucleation flux may be well represented by intermediate mixing concentrations with the phenomenological parameters β and γ.

The second point is the use of discrete fractions to represent a continuous flow. This is a standard practice and has been successfully used by Baldyga and Bourne (1984) and David and Villermaux (1987). We shall discuss in the next section how we can estimate the volumes V_A^* and V_B^* which may mix independently of the preceding and the succeeding fraction.

Comparison with Results from the Literature

When trying to compare predictions with results from the literature there arises the problem of estimating α. For semi-batch tanks it may be calculated as follows: Let t^f be the feeding time and V the initial volume in the tank. The experimental and theoretical results of Bourne and Dell'Ava (1987) show that molecular mixing is practically complete within one recirculation in the tank, that is, within circulation time t_c. The volume of reactant B which entered the precipitator during t_c is $Q_B^f t_c$ and thus we consider that this volume may mix independently of the preceding and succeeding fractions:

$$\alpha = \frac{V}{V_B^0} = \frac{V}{Q_B^f t_c} = \frac{t^f}{V_B^f t_c} \tag{20}$$

It should be noted that a consequence of this assumption is that at constant feed flow rate $V_B^0 \sim N^{-1}$. In the same way, α and m are proportional to N. For the case described by Tosun (1988), the parameter α is calculated as follows. The circulation time was evaluated in standard stirred tanks equipped with Rushton turbines by the correlation of Holmes et al. (1964)

$$t_c = 0.85(T/D)^2/N \tag{21}$$

between 0.42 and 4.2 s according to the minimum and maximum values of N (100 and 1,000 min^{-1} respectively).

Thus, with a 6 dm^3 tank simultaneously fed with two feed streams of 30 $\text{cm}^3 \cdot \text{min}^{-1}$ each:

$$2{,}850 \leq \alpha \leq 28{,}500$$

Similarly, we can derive for continuous stirred tanks of volume V with $Q_A^f = Q_B^f$:

$$\alpha = \frac{V}{V_B^0} = 2\,\frac{\tau}{t_c} \tag{22}$$

The experimental conditions of the different studies are listed in Table 1 and compared with the predictions of the model. The agreement is generally good. All these experiments are performed with equal flow rates and concentrations in both feed streams ($\delta = 1$) and symmetrical feeding.

Influence of feed location

In the study reported by Tosun (1988), feed location effects were observed in his double jet experiments on barium sulfate precipitation in a stirred tank with initial conditions: $\sigma^f = 10^{10}$, α between 2,850 and 28,500, and B_N probably about 220 at such high supersaturations (Dirksen and Ring, 1991; Nielsen, 1964). These conditions correspond to zone *a* at low stirring speeds and to zone *b* at high stirring speeds. In the experiments, a decrease in the average size was observed for the feed location CC (both inlet tubes close together and located in a highly turbulent region) as compared with location AA (feed tubes separated but also located both in a highly turbulent region). Moving the tubes from CC to AA may be interpreted as keeping β constant and reducing γ. Thus, the average size should increase (Figures 5 and 7) due to a smaller nucleation flux in both zones. This is in agreement with the experimental trend.

When changing from setup BB (distant feed tubes both located in a less turbulent region) to AA, a variable increase in average size was noted which became significant at high stirring speeds. This change from BB to AA may be interpreted as keeping γ constant but small, coupled with an increase of β. Thus, depending on the β value the average size may decrease or increase (Figures 4 and 6) as a consequence of the growth of both the criterion η and the nucleation flux ϕ. The decrease which is experimentally observed may be thus explained by the model if we assume β to be in the range >50.

The experimental observation that setups CC and DD gave different results at any stirring speed may be explained by the fact that the distance between the feed tubes was larger in the case DD than in the case CC. This may be again interpreted as being for constant β and lower γ in the case DD, leading to smaller average fluxes ϕ in both parametric zones.

Influence of stirring speed

Effects observed when the stirring speed N is varied at constant feed concentration and flow rates are less simple. First of all, modifications in stirring speed also affect other processes slower than primary nucleation: secondary nucleation, diffusion limited growth, agglomeration, breakage, which have contradictory effects on crystal number and size (Marcant and David, 1991). As far as primary nucleation is concerned, an increase in N leads mainly to an increase in β with almost constant γ for separated feed streams, and to a combined increase of both parameters for closer feed streams. This results in turn in an increase in η (see Figures 4 and 5) or at least in an intermediate maximum for η for higher β values. However, one should keep in mind that the parameter α depends on the stirring speed N through the circulation time t_c (Eqs. 20-21) since $t_c \sim N^{-1}$ (Holmes and Van Voncken, 1964) and it proportionally increases with N. Figure 3 shows that such an α increase leads to higher values of criterion η.

In addition, the reference supersaturation σ° also depends on α. For $\delta = 1$, we derive the following from Eqs. 2, 14 and 19:

$$\sigma^\circ = \frac{(\sqrt{\sigma^f} + \alpha)^2}{(2+\alpha)^2} \tag{23}$$

and since σ^f is high, σ° decreases with increasing α.

Thus, following Eq. 11, the reference nucleation flux ϕ° generally decreases. The total nucleation flux for the entire feed stock is written:

$$\Phi = \sum_{j=1}^{m} \phi = \sum_{j=1}^{m} (A_N V_B^0 \eta + \phi^\circ) \tag{24}$$

and the overall trend finally depends on the relative values of η and ϕ°.

If we are in zone b under conditions with large positive values of η, the variations of ϕ° can be neglected. V_B^0 varies as N^{-1}, but the number m of fractions increases accordingly with N. Thus, it is likely that globally Φ increases with N. Conversely, no definite conclusion can be drawn for Φ in the a zone because ϕ° is not negligible. The results of Tosun (1988) show complex effects of stirring speed; this may be a consequence of working between zone a and zone b conditions.

Influence of space time

A third attempt to test the model can be made by varying the space time τ in continuous stirred tank precipitators. In these experiments σ^f, γ and β are kept constant, but α (see formula 22) increases with τ, and consequently σ° decreases. In zone b, ϕ° is still negligible and the α increase makes up for the higher primary nucleation flux. In zone a, no obvious conclusion may be drawn for the same reason as above. It should also be noted that, as far as crystal size is concerned, other phenomena like secondary nucleation, diffusional growth or agglomeration may interplay with primary nucleation.

All these considerations may explain that some very different and sometimes contradictory behavior has been observed for the effect on crystal sizes of increasing the stirring speed during double-jet precipitation of barium sulphate (Pohorecki and Baldyga, 1988; Tosun, 1988; Fitchett and Tarbell, 1990). Furthermore, some experimental parameters (α, for instance) were difficult to recalculate accurately. We therefore decided to perform our own experiments (Marcant, 1992), using calcium oxalate monohydrate (COM) precipitation, which had been successfully used for single-jet precipitation (Marcant and David, 1991). The fact that significant agglomeration takes place during COM precipitation is not an obstacle for studying mixing effects induced by primary nucleation, because it has been shown (David and Marcant, 1991) that the effects of agglomeration as well as growth on crystal-size distribution are the same for all feed locations. Consequently, variations of crystal-size distribution which may be observed when changing the location of feed streams are caused by the interaction of primary nucleation and micromixing.

Experiments

The semibatch double jet precipitation setup is described in Figure 8. A semibatch precipitator was preferred to avoid scaling which appears during long runs. Both injectors are located within the tank with an accuracy of ± 1 mm on the three coordinates. The tank initially contains pure water and reaches a final volume V_{end} of 1.5 dm^3. We define:

$$\alpha' = \frac{\text{initial volume}}{\text{sum of volumes fed to the tank}} = \frac{V}{V_A^f + V_B^f} \tag{25}$$

α' is varied between 4 and 48. In our experiments, $V_A^f = V_B^f$.

The flow rates of both feeds are kept equal in the range 0.6–0.8 cm$^3 \cdot$s^{-1}. We define two other new mixing concentrations $C_A'^\circ$ and $C_B'^\circ$ of the entire feedstocks with the bulk but without reaction that were fixed to 10 mol$\cdot$m^{-3} for both calcium and oxalate. Two couples of feed points were selected according to Tosun (1988) and named AA and BB, respectively. σ^f is evaluated from the feed concentrations:

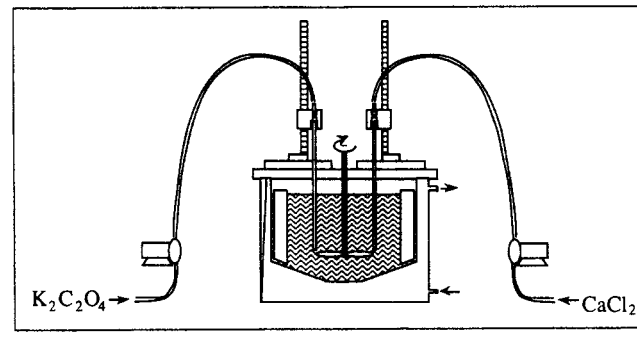

Figure 8. Experimental apparatus for double jet precipitation experiments with feed locations AA.

$$C_B^f = \frac{C_B'^\circ V_{end}}{V_B^f} = 2C_B'^\circ (1+\alpha') \tag{26}$$

$$\sigma^f = 4(1+\alpha')^2 \frac{C_A'^\circ C_B'^\circ}{P_S} \tag{27}$$

As the precipitation is very fast, it is not easy to monitor the concentrations of reactants and thus their rate of conversion. Only the final crystal-size distribution was measured by taking samples out of the final suspension. These samples were analyzed by a Malvern Mastersizer laser diffraction particle sizer. The results are reported as the volume weighted average size L_{43}. The accuracy on L_{43} was estimated to be about ± 0.3 μm.

X-ray diffractograms and SEM observations showed that the precipitates consisted of a mixture of calcium oxalate monohydrate (COM) mainly, dihydrate (COD) with a small proportion of trihydrate (COT), whereas only COM was produced during our previous batch experiments (Marcant and David, 1991).

Before discussing the results, we must first relate the model parameters α, σ^f and B to the experimental conditions.

Parameter α is calculated from α'. From Eq. 20, we derive:

$$\alpha = \frac{2\alpha' V_B^f}{Q_B^f t_c} \tag{28}$$

since $\delta = 1$:

$$V_B^f = \frac{V_{end}}{(2+2\alpha')} \tag{29}$$

and

$$\alpha = \frac{\alpha' V_{end}}{Q_B^f t_c (1+\alpha')} \tag{30}$$

For $\alpha' = 4$, $t_c = 0.6$–2.4 s (according to N), $V_{end} = 1.5$ dm^3, $Q_B^f = 0.7$ cm$^3 \cdot$s^{-1}: $\alpha = 710$–$2{,}850$, while for $\alpha' = 48$ and same t_c, V_{end}, Q_B^f: $\alpha = 825$–$3{,}300$.

Note that α slightly depends on α'.

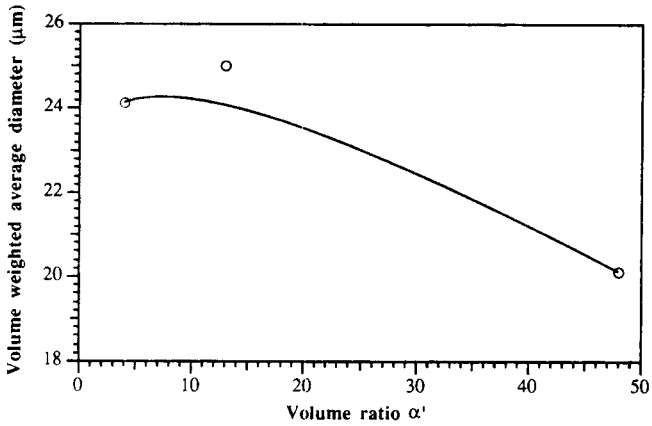

Figure 9. Influence of volume ratio α' on final volume weighted average size L_{43}.

$C_A'^\circ = C_B'^\circ = 10$ mol·m^{-3}; $Q_B^f = 0.7$ cm^3·s^{-1}; $N = 10$ s^{-1}; feed locations AA.

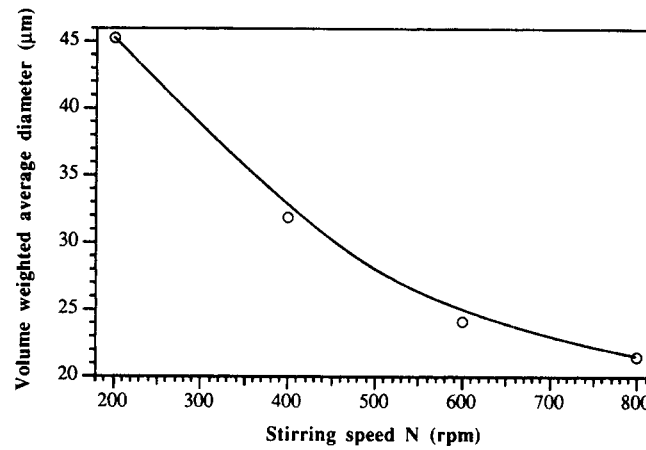

Figure 10. Influence of stirring speed on final volume weighted average size L_{43}.

Same conditions as for Figure 8; $\alpha' = 4$.

We took $P_S = 1.7\ 10^{-3}$ mol^2·m^{-6} which is the COM value as the solubilities of all the hydrates are of the same order of magnitude and because the COM is the most stable product.

From Eq. 27, we deduce that σ^f varies between $4 \cdot 10^6$ and $6 \cdot 10^8$.

Finally, assuming that the kinetic studies of Marcant (1992) are valid, we have $B_N = 70$. The values of α, σ^f and B_N indicate that the model operates in zone b.

Results and Discussion

In a first set of experiments, α' was varied (Figure 9) with feed location AA and constant total amount of both reactants and same flow rates. The general experimental tendency is that the volume averaged size L_{43} falls when α' increases. However, such experimental conditions may lead to changes of supersaturation profiles against time, so that all elementary processes may be influenced.

As far as the primary nucleation is concerned, since the same amounts of both reactants are mixed, that is, $C_A'^\circ$ and $C_B'^\circ$ are constant, the increase in α' leads to constant α according to Eq. 30 and to a large σ^f increase according to Eq. 27. Consequently, the model (Figure 3) indicates that we move towards zero η values by increasing α'. However, according to Eq. 23 σ° also increases sharply and subsequently ϕ° as well. When η becomes very small, the ϕ° effect makes up for ϕ (see formula 24). The number of fractions m is also increased. Thus, the nucleation flux is likely to increase, which seems to agree with the experimental observations.

In a second set of experiments, the stirring speed was varied from 200 up to 800 min^{-1} (Figure 10). In this case, the volume weighted average size L_{43} sharply decreases. Note that L_{43} is divided by a factor 2 between the extreme N values.

As stated previously, it is difficult to interpret these experimental results because of the multiple consequences of a change in stirring speed on primary and secondary nucleation, diffusional growth and agglomeration. As the two last phenomena result in size increase at higher stirring speeds (Marcant and David, 1991), it is likely that the nucleation phenomena, that is, primary and secondary nucleation, which both act in the opposite direction, are predominant. Tosun (1988) had already observed a minimum with the same kind of experiments under zone b conditions (Table 1), but he explored a wider range of stirring speeds (between 100 and 1,000 min^{-1}) than used in the present work.

In this second series of experiments, α', but not α, σ^f and B_N, are constant. As we still are in zone b, according to the model, and as discussed in the preceeding section, the total nucleation flux Φ should increase with N. If this primary nucleation phenomenon is determinant for crystal size, the average size L_{43} should decrease. This is observed in the experiments, as shown in Figure 10.

The third set of experiments (Figure 11) is the simplest to discuss. Both couples of feed points AA and BB were used at two different stirring speeds. Obviously, no decisive change of L_{43} could be noticed by switching from AA to BB location. Here, α, σ°, σ^f and B_N are all constant because N and α' are constant. As explained above and in Table 1, such a change of feeding may be interpreted as having β increasing from BB to AA and γ being kept small and constant. Figure 6 indicates that in zone b, both η and ϕ should increase or decrease slightly, depending on the value of β. These predictions correspond to the experimental figures. Note that Tosun (1988) already ob-

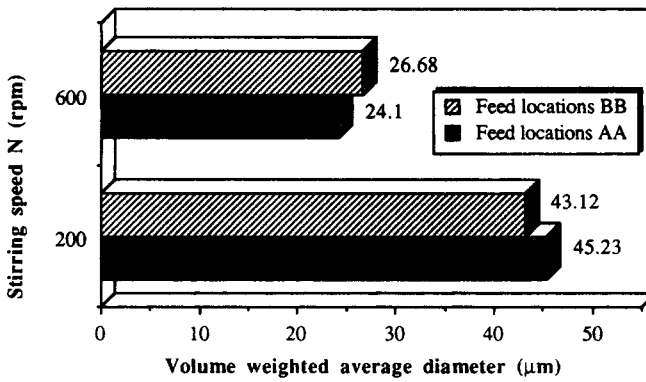

Figure 11. Influence of feed locations on final volume weighted average size L_{43} at two different stirring speeds.

Same conditions as for Figure 9.

served miscellaneous effects on the average size for similar experiments.

Conclusion

In summary, two out of three sets of calcium oxalate precipitations in double-jet semibatch configuration yielded results in good qualitative agreement with our model. This agreement also seems to be satisfactory in the case of variation of volume ratio α' or stirring speed N, but the analysis is complicated due to the multiplicity of effects caused by the stirring speed. Finally, changes in feed location showed weak micromixing effects for the double-jet precipitation of calcium oxalate, which were quite different from the sharp effects observed in the same case using single-jet precipitation.

However, a general issue is that there are at least two types of precipitations which differ by the values of the parameters α (feed rate compared to recycled rate), σ^f (initial supersaturation) and B_N (stiffness of primary nucleation rate). In the first zone (a) the actual nucleation flux ϕ is less than the reference flux ϕ° which would result from perfect and instantaneous mixing in the tank; in the second case (zone b), ϕ becomes higher than ϕ°. This may lead to different behaviors when changing physical or mechanical parameters, as noted by several authors.

The multiplicity of physical and operational parameters makes the modeling of double jet precipitation accompanied by mixing effects very difficult indeed. Thus, when compared with single-jet precipitation, double-jet precipitation is not so well suited for studying micromixing effects. As a consequence, the degree of refinement of mixing models used for this purpose should be restricted to a minimum so as to avoid too much additional complexity.

Acknowledgment

The authors are indebted to Rhône-Poulenc Industrialisation for financial support of this work.

Notation

A_N = nucleation rate constant, number of crystals$\cdot m^{-3}\cdot s^{-1}$
B_N = nucleation rate activation factor
C = concentration, mol$\cdot m^{-3}$
D = stirrer diameter, m
L_{43} = volume weighted average size, m
m = number of feed fractions
N = stirring speed, s^{-1}
P_S = solubility product, mol$^2\cdot m^{-6}$
Q = volumetric flow rate, $m^3\cdot s^{-1}$
r_N = nucleation rate, number of crystals$\cdot m^{-3}\cdot s^{-1}$
t_c = circulation time, s
t^f = feeding time, s
T = tank diameter, m
V = initial volume, m^3
V_A^0 = A initial fraction volume, m^3
V_B^0 = B initial fraction volume, m^3
V_{end} = volume after end of addition, m^3

Greek letters

α = ratio between fresh fluid volume V_B^0 and volume of the bulk
α' = ratio of initial volume V to sum of feed volumes $V_A^f + V_B^f$
β = volume ratio between bulk fluid and fresh fluid mixed, Figure 2
γ = fraction of fresh fluid volume V_B^0 directly mixed with a fraction of V_A^0, Figure 2
δ = flow rate ratio between both feed streams, $= V_A^0/V_B^0$
η = primary nucleation flux criterion
σ = supersaturation ratio
τ = space time, s
ϕ = nucleation flux (number of crystals$\cdot s^{-1}$)
Φ = total nucleation flux corresponding to the entire feedstocks (number of crystals$\cdot s^{-1}$)

Subscripts

A = reactant A
B = reactant B
I, II, III = subregions I, II and III

Superscripts

b = bulk conditions
f = feed conditions
$^\circ$ = perfect mixing conditions, after mixing $V_B^0 + V_A^0$ with the bulk
0 = initial conditions
$'^\circ$ = perfect mixing conditions, both entire feedstocks mixed with initial volume

Literature Cited

Baldyga, J., and J. R. Bourne, "A Fluid Mechanical Approach to Turbulent Mixing and Chemical Reaction," *Chem. Eng. Commun.*, **28**, 231 (1984).

Bourne, J. R., and P. Dell'Ava, "Micro- and Macro-mixing in Stirred Tank Reactors of Different Sizes," *Chem. Eng. Res. Des.*, **65**, 180 (1987).

David, R., and J. Villermaux, "Interpretation of Micromixing Effects on Fast Consecutive-Competing Reactions in Semi-batch Stirred Tanks by a Simple Interaction Model," *Chem. Eng. Commun.*, **54**, 333 (1987).

Dirksen, J. A., and T. A. Ring, "Fundamentals of Crystallization: Kinetic Effects on Particle Size Distributions and Morphology," *Chem. Eng. Sci.*, **46**, 2389 (1991).

Fitchett, D. E., and J. M. Tarbell, "Effect of Mixing on the Precipitation of Barium Sulfate in a MSMPR Reactor," *AIChE J.*, **36**, 511 (1990).

Holmes, D. B., R. M. Van Voncken, and J. A. Dekker, "Fluid Flow in Turbine-Stirred Baffled Tanks," *Chem. Eng. Sci.*, **19**, 201 (1964).

Kuboi, R., M. Harada, J. M. Winterbottom, A. J. S. Anderson, and A. W. Nienow, "Mixing Effects in Double-Jet and Single-Jet Precipitation," World Congress III of Chemical Engineering, Tokyo, paper 8g-302, Vol. II, pp. 1040 (1986).

Marcant, B., and R. David, "Experimental Evidence for and Prediction of Micromixing Effects in Precipitation," *AIChE J.*, **37**, 1698 (1991).

Marcant, B., "Méthodologie d'Analyse d'un Système de Précipitation Soumis à l'Influence des Conditions de Mélange: Cas de l'Oxalate de Calcium," PhD thesis, INPL, Nancy, France (1992).

Mydlarz, J., J. Reber, D. Briedis, and J. A. Voigt, "Kinetics of Zinc Oxalate Precipitation in a Mininucleator—MSMPR Crystallizer System," AIChE. Symp. Ser., **87**, 158 (1992).

Nielsen, A E., "Homogeneous Nucleation in Barium Sulphate Precipitation," *Acta Chemica Scandinavica*, **15**, 441 (1961).

Pohorecki, R., and J. Baldyga, "The Effects of Micromixing and the Manner of Reactor Feeding on Precipitation in Stirred Tank Reactors," *Chem. Eng. Sci.*, **43**, 1949 (1988).

Tosun, G., "An Experimental Study of the Effect of Mixing Intensity on Particle Size Distribution in Barium Sulfate Precipitation Reaction," 6th European Conference on Mixing, Pavia, Italy, p. 161 (1988).

Volmer, M., and A. Weber, "Keimbildung in übersättigten Gebilden," *Z. Phys. Chem.*, **119**, 277 (1926).

Manuscript received Jan. 28, 1993, and revision received July 19, 1993.